The outer segment serves as a default destination for the trafficking of membrane proteins in photoreceptors

Sheila A. Baker,[1] Mohammad Haeri,[2] Peter Yoo,[1] Sidney M. Gospe III,[1] Nikolai P. Skiba,[1] Barry E. Knox,[2] and Vadim Y. Arshavsky[1]

[1]Albert Eye Research Institute, Duke University Medical Center, Durham, NC 27710
[2]Department of Biochemistry and Molecular Biology and Ophthalmology, State University of New York, Upstate Medical University, Syracuse, NY 13210

Photoreceptors are compartmentalized neurons in which all proteins responsible for evoking visual signals are confined to the outer segment. Yet, the mechanisms responsible for establishing and maintaining photoreceptor compartmentalization are poorly understood. Here we investigated the targeting of two related membrane proteins, R9AP and syntaxin 3, one residing within and the other excluded from the outer segment. Surprisingly, we have found that only syntaxin 3 has targeting information encoded in its sequence and its removal redirects this protein to the outer segment. Furthermore, proteins residing in the endoplasmic reticulum and mitochondria were similarly redirected to the outer segment after removing their targeting signals. This reveals a pattern where membrane proteins lacking specific targeting information are delivered to the outer segment, which is likely to reflect the enormous appetite of this organelle for new material necessitated by its constant renewal. This also implies that every protein residing outside the outer segment must have a means to avoid this "default" trafficking flow.

Introduction

Normal vision is dependent on the function of rod and cone photoreceptors, which are sensory neurons proven to be among the most productive model systems for studying signal transduction and sensory physiology. The key feature that makes them so amenable is their highly compartmentalized organization. Photoreceptors consist of four major compartments: a photosensitive outer segment containing highly packed disc membranes and the proteins required to initiate a response to light, an inner segment where proteins and lipids are synthesized and energy is produced, a nuclear region, and a synaptic terminal that sends information to the second order neurons in the retina (for reviews see Papermaster, 2002; Williams, 2004). To establish this polarization, photoreceptors need to tightly control the subcellular targeting of many newly synthesized proteins. As in other cells, protein segregation into distinct membrane compartments requires regulated sorting in the ER and Golgi followed by vesicular trafficking to final destinations. The importance of correct protein targeting in photoreceptors is highlighted by the observations that mutations in targeting signals or trafficking machinery cause degenerative diseases. However, specific targeting information has been revealed for only a handful of photoreceptor-specific proteins, with most of the emphasis on rhodopsin.

One interesting aspect of photoreceptor compartmentalization is that its electrically continuous plasma membrane is separated by a diffusional barrier into two domains with distinct protein compositions, one representing the outer segment and another the rest of the cell. Notably, the densely packed discs comprising the majority of outer segment membranes are formed inside the outer segment by evaginations of the plasma membrane, requiring all disc-specific proteins to be first targeted to the outer segment compartment of the plasma membrane (Steinberg et al., 1980). By analogy with other polarized cells (for reviews see Mostov et al., 2003; Muth and Caplan, 2003; Rodriguez-Boulan and Musch, 2005),

Correspondence to Vadim Y. Arshavsky: vadim.arshavsky@duke.edu

Abbreviation used in this paper: mGluR1, metabotropic glutamate receptor 1.

The online version of this article contains supplemental material.

Supplemental material can be found at:
http://doi.org/10.1083/jcb.200806009

The Rockefeller University Press $30.00
J. Cell Biol. Vol. 183 No. 3 485–498
www.jcb.org/cgi/doi/10.1083/jcb.200806009

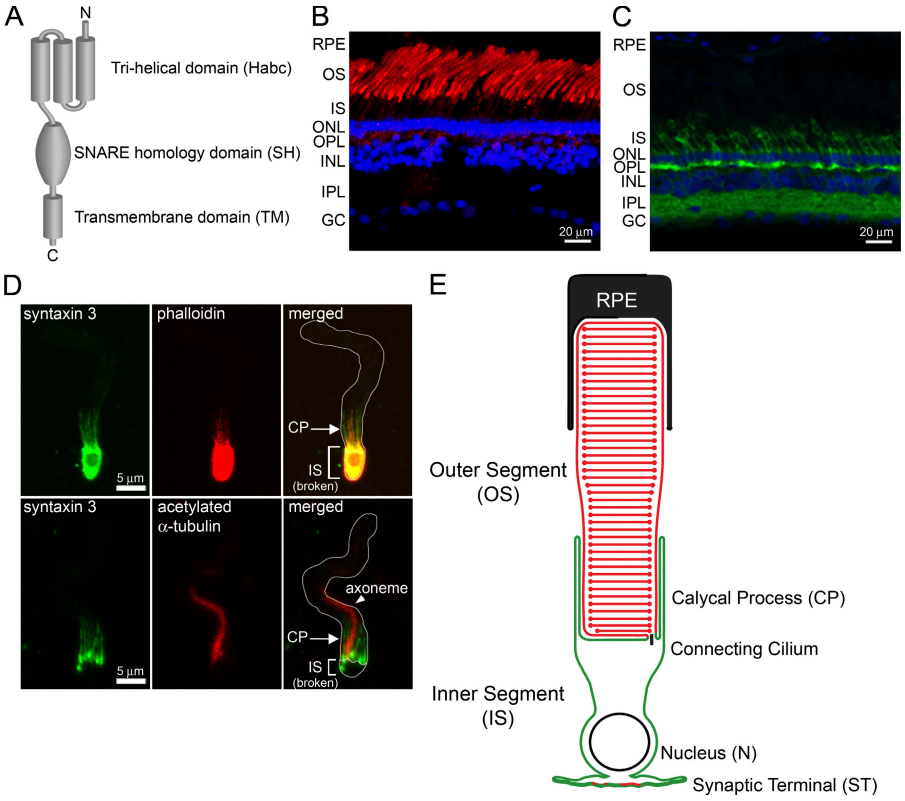

Figure 1. **Localization of R9AP and syntaxin 3 in *Xenopus* photoreceptors.** (A) Domain organization shared by R9AP and syntaxin 3. Both contain an N-terminal Habc domain, a SNARE homology domain, and a C-terminal transmembrane domain. (B) Immunofluorescence of R9AP (red) using the antibody against xR9AP2 in rod and cone outer segments of adult *Xenopus* retina. (C) Immunostaining of syntaxin 3 (green) in adult *Xenopus* retina. (B and C) The nuclei are counterstained with Hoechsts (blue). RPE, retinal pigmented epithelium; OS, outer segment; IS, inner segment; ONL, outer nuclear layer; OPL, outer plexiform layer; INL, inner nuclear layer; IPL, inner plexiform layer; GC, ganglion cell. No signals were revealed in controls where the primary antibodies were omitted. (D) Immunostaining of syntaxin 3 (green) in two examples of broken rod outer/inner segment preparations double labeled either with phalloidin (red; top), which labels the actin-rich calycal processes (CP), or with acetylated α-tubulin (red; bottom), which labels the axoneme within the connecting cilium and the outer segment. The right panels are the merged image with the shape of the entire cell fragment outlined in white, as seen in the transmitted light channel. Note that multiple calycal processes are seen as the image is a z-stack projection. (E) Cartoon of the rod photoreceptor with the regions containing R9AP in red and the regions containing syntaxin 3 outlined in green.

it is likely that membrane proteins residing in each compartment are delivered by separate trafficking pathways and encode distinct targeting sequences that identify which of these pathways will be used. Indeed, two targeting signals responsible for directing membrane proteins to the outer segment have been identified. One motif is shared by rhodopsin, cone opsins, and photoreceptor-specific retinol dehydrogenase (Deretic et al., 1998; Tam et al., 2000; Luo et al., 2004) and the second is found in RDS/peripherin 2 (Tam et al., 2004). However, these targeting signals are not present in any other membrane proteins resident in the outer segment and virtually nothing is known about protein targeting to the rest of the plasma membrane.

The goal of this study was to understand the differential targeting of two proteins, which are very similar structurally yet reside in the two separate membrane compartments. One was R9AP, which resides primarily in the outer segment, both in the plasma membrane and the photoreceptor discs. R9AP's function is to anchor the GTPase-activating complex, which sets the duration of rods' and cones' response to light (Hu and Wensel, 2002). The second protein was syntaxin 3, which is a plasma membrane protein excluded from the outer segment and enriched at the synaptic terminal. Its function is to serve as a target membrane component of the SNARE complex mediating vesicular fusion (for review see Hay, 2001). Our approach took advantage of the experimental model of transgenic *Xenopus laevis* (Knox et al., 1998; Amaya and Kroll, 1999; Tam et al., 2000). We analyzed a series of each protein's mutants and chimeric constructs expressed as transgenes in *Xenopus* rods to determine the sequence information that governs the differential targeting of each protein.

Surprisingly, we have found that only one of these proteins, syntaxin 3, has targeting information encoded in its sequence. In the case of R9AP, all that is needed to get primarily to the outer segment is its transmembrane domain, which is not a sequence-specific signal. Furthermore, removing the information defining the cellular localization from syntaxin 3 redirected its localization primarily to the outer segment. This was also true for two other proteins we tested, normally residing in mitochondria or the ER; depriving them of specific targeting information redirected them to the outer segment as well. These findings reveal a pattern in which proteins lacking specific targeting sequences are delivered predominantly to the outer segment. This "default" targeting is so efficient that even key signaling proteins, such as R9AP, may reach the photoreceptor outer segment, which is traditionally viewed as a privileged cellular destination, in the absence of a targeting signal.

Results

Differential subcellular localization of R9AP and syntaxin 3 in frog photoreceptors

R9AP and syntaxin 3 are tail-anchored transmembrane proteins sharing a great degree of structural similarity (Keresztes et al., 2003; Martemyanov et al., 2003; Sharma et al., 2006). Each contains an N-terminal trihelical bundle, called the Habc domain in syntaxins, followed by the SNARE homology domain and the C-terminal transmembrane domain (Fig. 1 A). Their subcellular localization patterns are distinctly different in mammalian rods (Morgans et al., 1996; Hu and Wensel, 2002; Keresztes et al., 2003; Martemyanov et al., 2003; Sherry et al., 2006; Chuang et al., 2007) and we confirmed this in the frog retina

(Fig. 1, B and C). R9AP was found primarily in rod and cone outer segments with a small fraction in synaptic terminals, as in other species (Fig. 1 B). Syntaxin 3 is present in both photoreceptors and the inner retina (Fig. 1 C). Within photoreceptors, it was found throughout the entire membrane of the inner segment with enrichment in synaptic terminals, but was notably absent in the outer segments. A recent study reported that in mouse photoreceptors syntaxin 3 labeling could be detected within the base of the outer segment (Chuang et al., 2007). We examined this region in the frog photoreceptor, which is best labeled by the antibody in a broken rod preparation containing the outer segment and a fragment of the inner segment (Kaplan et al., 1987), and observed robust syntaxin 3 immunostaining in the remaining portion of the inner segment and in the inner segment calycal processes surrounding the base of the outer segment, but no staining beyond this junction (Fig. 1 D).

Therefore, R9AP and syntaxin 3 could be used as markers for distinct membrane domains in photoreceptors. Our strategy in identifying the sequence information required for each of them to reach their corresponding subcellular destinations was to first perform a deletion mutagenesis on each protein individually and then to analyze the localization of chimeric constructs containing various combinations of R9AP and syntaxin 3 domains. But before presenting the analysis of the targeting information coded in their sequences, we describe how we identified the *Xenopus* homologues of these proteins to use in this study. The National Center for Biotechnology Information database contains a single *Xenopus* homologue for syntaxin 3 (Gene ID 444751) and this sequence was used in our experiments. However, the identification of the photoreceptor-specific R9AP required additional analysis.

Identification of the photoreceptor-specific R9AP isoform in *Xenopus*

Unlike mammals, frogs have two genes homologous to R9AP (Fig. 2 A). We termed the first gene xR9AP1 (Gene ID 494990) because it is more similar to the mammalian R9AP gene (62% identical to mouse R9AP) and the second gene xR9AP2 (Gene ID 444631; 47% identical to mouse R9AP). To determine which one is expressed in rods, we first used RT-PCR on DNase-treated RNA isolated from *Xenopus* retina and found that both R9AP transcripts are present (Fig. 2 B). We next raised antibodies against each R9AP protein and found that the anti-xR9AP2 antibody recognized a robust doublet at the predicted molecular mass of 27 kD in the membrane fraction of *Xenopus* retina homogenate (Fig. 2 C), whereas the anti-xR9AP1 antibody showed no signal in the predicted molecular mass range (not depicted). Finally, we coimmunoprecipitated R9AP from frog retinas using antibodies against its photoreceptor-specific partner, RGS9-1, and confirmed the identity of the coprecipitating protein as xR9AP2 but not xR9AP1 by both Western blotting (Fig. 2 D) and mass spectrometry sequencing (not depicted). Although we cannot entirely exclude the possibility that low undetectable amounts of xR9AP1 are present in frog photoreceptors, we conclude that xR9AP2 is the major R9AP isoform in frog photoreceptors and we used it for the remainder of the study. For simplicity, we refer to it as R9AP from here on.

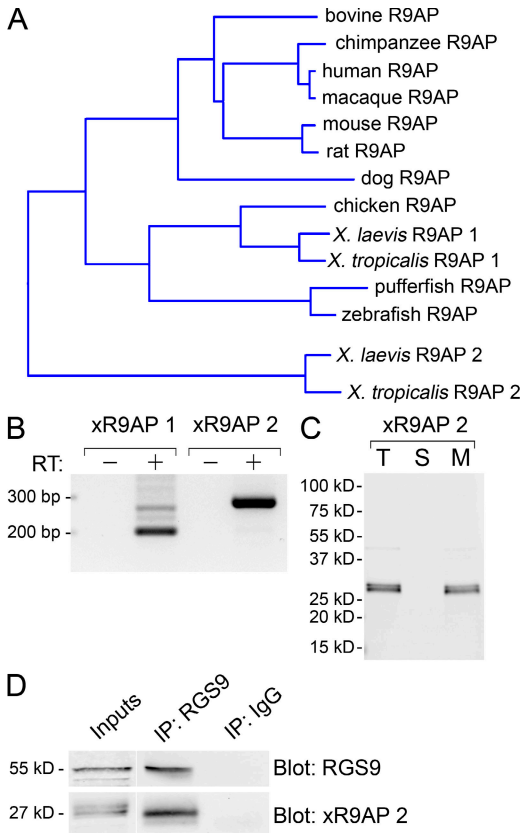

Figure 2. **Identification of the photoreceptor-specific R9AP isoform in *Xenopus*.** (A) Phylogeny tree of R9AP protein sequences built using the Neighbor-Joining method. Accession nos. are as follows: bovine, AAM67417; chicken, NP_989836; chimpanzee, XP_512566; dog, XP_855518; human, NP_997274; macaque, XP_001087093; mouse, NP_665839; pufferfish, CAF92756; rat, XP_001079782; zebrafish, XP_687644. *Xenopus tropicalis* R9AP1 is deduced from genome v4.1, scaffold 94 (920566:921276), and *X. tropicalis* R9AP2 is deduced from genome v4.1, scaffold 761 (402303:408685). (B) RT-PCR amplification of xR9AP1 and xR9AP2 transcripts from *Xenopus* retina; omission of reverse transcription (RT) in parallel samples served as a negative control for DNA contamination. (C) Western blot of *Xenopus* retina extract probed with the antibody specific to xR9AP2. Lane T, total extract; lane S; soluble protein fraction; lane M, membrane fraction. Note that the xR9AP2 band is a doublet, which reflects the previously documented phosphorylation of R9AP in photoreceptors (Martemyanov et al., 2003). (D) xR9AP2 coimmunoprecipitates with RGS9-1 from *Xenopus* retina. Beads coated with sheep IgG were used for the negative control.

The transmembrane domain of R9AP is sufficient for outer segment targeting

We first identified the regions of R9AP required for its targeting to rod outer segments. A series of R9AP fragments were fused to GFP and expressed under the rod-specific rhodopsin promoter (Knox et al., 1998); a summary of all transgenically expressed proteins used in this study is shown in Table I. To establish the baseline, we studied the distribution of full-length R9AP, which was found to be similar to that of the endogenous protein (Fig. 3 A). The majority of GFP signal originated from the outer segment, with some also detected in the synaptic terminal and plasma membrane of the rod. Note that the GFP signal in the outer segments often appears as distinct bands of various thicknesses and that the transgene expression is mosaic from cell to cell. This phenomenon has

Table I. **Summary of all transgenic constructs presented in this study**

Construct	Cartoon	Primary localization	Figure
GFP		IS, soluble	Fig. 5 A
GFP-R9AP		OS	Fig. 3 A and Fig. 10
GFP-R9APΔHabc		OS	Fig. 3 B
GFP-R9APΔSH		OS	Fig. 3 C
GFP-R9AP TM	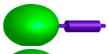	OS	Fig. 3 D and Fig. 9 A
GFP-R9APΔTM		IS, soluble	Fig. 3 E
GFP-R9AP TM shorter (−2 aa)	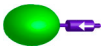	OS and IS	Fig. 9 B
GFP-R9AP TM shortest (−4 aa)		IS	Fig. 9 C
Myc-R9AP		OS	Fig. 6 A and Fig. S1 A
Myc-R9AP TM shorter (−2 aa)		OS and IS	Fig. S3
Myc-R9APΔHabc		OS	Fig. S1 B
Myc-R9APΔSH		OS	Fig. S1 C
GFP-mGluR1 TM 1	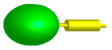	OS	Fig. 7
GFP-Cyt b5 TM	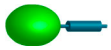	ER	Fig. 8 A and Fig. S2
GFP-Cyt b5 TM longer (+4 aa)	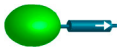	OS	Fig. 8 B
GFP-BclXL TM	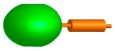	MT	Fig. 8 C
GFP-BclXL TM K233S	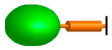	OS and IS	Fig. 8 D
GFP-BclXL TM, K233S, longer (+4 aa)	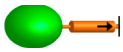	OS	Fig. 8 E
GFP-Stx 3	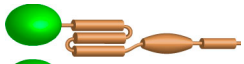	ISPM	Fig. 4 A
GFP-Stx $3_{(FMDE-AAAA)}$	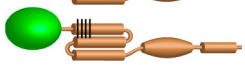	ISPM	Fig. 4 E
GFP-Stx 3ΔHabc	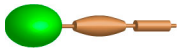	ISPM and IS	Fig. 4 B
GFP-Stx 3ΔSH		OS and ISPM	Fig. 4 C
GFP-Stx 3 TM	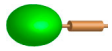	OS	Fig. 4 D and Fig. 10
GFP-Stx 3ΔTM	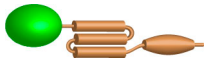	IS, soluble	Fig. 5 C
GFP-Stx 3ΔTM gg	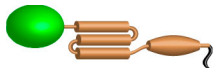	ISPM	Fig. 5 F
GFP-Stx 3 Habc	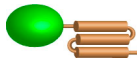	IS, soluble	Fig. 5 B
GFP-Stx 3 Habc gg	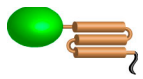	OS	Fig. 5 E
Myc-Stx 3		ISPM	Fig. 6 B
Myc-R9AP/Stx $3_{(TM)}$		OS	Fig. 6 C
Myc-Stx 3/$R9AP_{(SH)}$		OS	Fig. 6 D
Myc-Stx 3/$R9AP_{(TM)}$	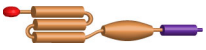	OS	Fig. 6 E
Myc-R9AP/Stx $3_{(SH)}$	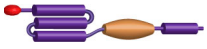	IS	Fig. 6 F

ER, endoplasmic reticulum; gg, geranylgeranylated; IS, inner segment; ISPM; inner segment plasma membrane, MT, mitochondria; OS, outer segment.

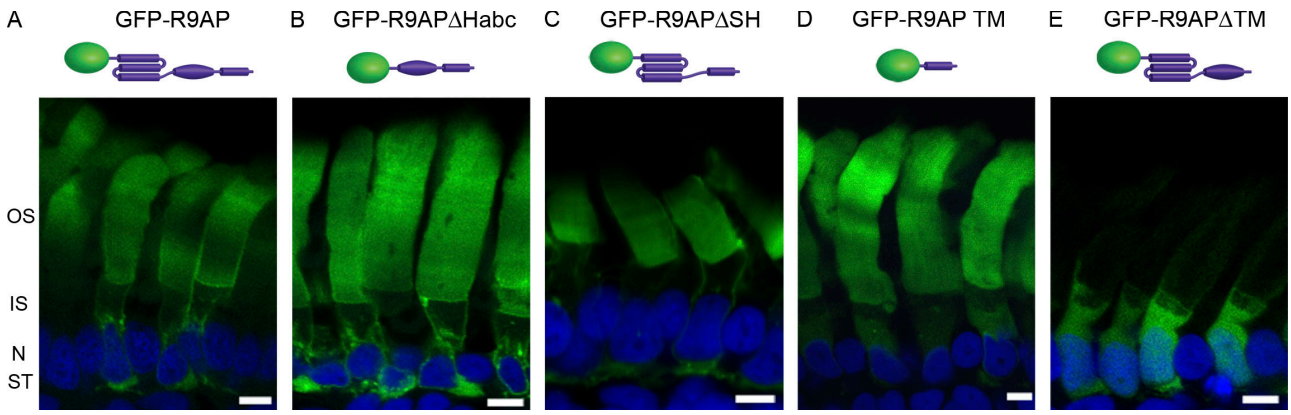

Figure 3. **Localization of GFP-tagged R9AP and R9AP mutants in transgenic *Xenopus* rods.** The following constructs were expressed in transgenic *Xenopus* rods: full-length GFP-tagged R9AP (A), GFP-tagged R9AP lacking the Habc domain (B), and GFP-tagged R9AP lacking the SNARE homology (SH) domain (C). (D) GFP-tagged transmembrane domain from R9AP. (E) GFP-tagged R9AP lacking the transmembrane domain. In all panels nuclei are counterstained with Hoechsts (blue). OS, outer segment; IS, inner segment; N, outer nuclear layer; ST, synaptic terminal. Bars, 5 µm.

been consistently seen in all previously published studies using the same promoter, although the underlying mechanisms are not well-understood (Moritz et al., 2001b). In addition, we observed that this protein construct had a propensity to form aggresomes in the inner segment above the nucleus. We tested whether the latter may reflect the relatively large GFP portion of the molecule interfering with the proper folding of the R9AP molecule by substituting GFP for a small Myc epitope tag (Fig. S1 A, available at http://www.jcb.org/cgi/content/full/jcb.200806009/DC1; and see Fig. 5 E). Indeed, this resulted in far fewer aggresomes with the majority of Myc-R9AP detected in the outer segment and a low level of signal found in the synaptic terminal as is the case with endogenous R9AP. Note that the overexpression of R9AP or any of the other proteins we expressed in transgenic rods in the course of this study did not result in any signs of retinal cell death.

The data shown in Fig. 3 (B–D) demonstrate that the pattern of R9AP distribution remains essentially unchanged in a series of deletion mutants lacking either some or all of its cytoplasmic domains. As in the case of full-length R9AP, we also tested two Myc-tagged R9AP deletion mutants and found no difference between the targeting of these molecules and the GFP-tagged variants (Fig. S1, B and C). Finally, removal of the transmembrane domain from GFP-R9AP resulted in a soluble protein localized primarily to the inner segment (Fig. 3 E), including the nucleoplasmic space, in a pattern indistinguishable from that of GFP alone (see Fig. 5 A; Knox et al., 1998; Peet et al., 2004). Overall, these data indicate that the transmembrane domain of R9AP is both necessary and sufficient to achieve outer segment localization.

The subcellular localization of syntaxin 3 requires the SNARE domain

We next conducted a similar deletion mutagenesis with syntaxin 3 constructs. First, we looked at the full-length GFP-tagged *Xenopus* syntaxin 3 (Fig. 4 A) and found its subcellular localization pattern to be the same as that of the endogenous protein (Fig. 1, C and D). The deletion of the N-terminal Habc domain did not cause a major change in the localization pattern, except that a larger fraction of the expressed construct

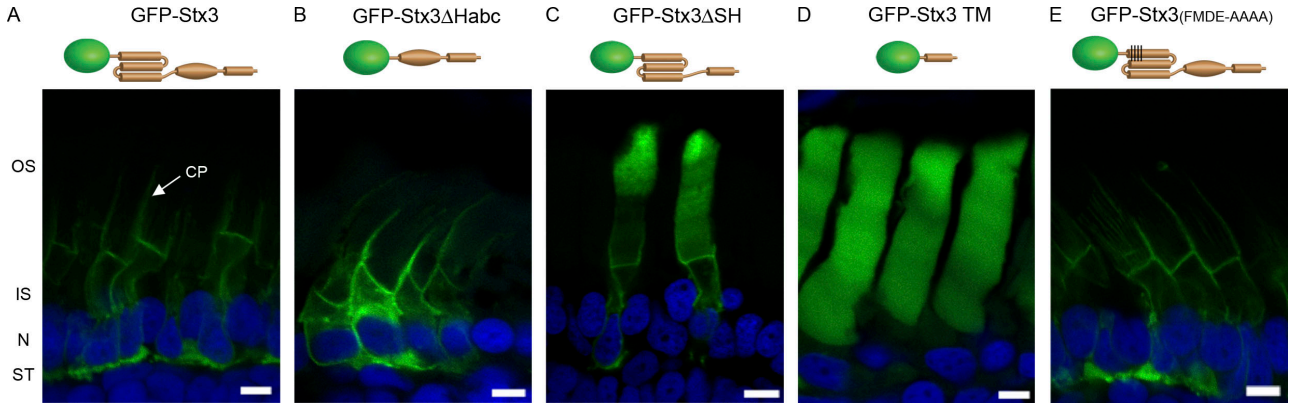

Figure 4. **Localization of GFP-tagged syntaxin 3 and syntaxin 3 mutants in transgenic *Xenopus* rods.** (A) Full-length GFP-tagged syntaxin 3 (Stx3). The arrow indicates the calycal processes (CP). (B) GFP-tagged syntaxin 3 lacking the Habc domain. (C) GFP-tagged syntaxin 3 lacking the SNARE homology domain. (D) GFP-tagged transmembrane domain from syntaxin 3. (E) Full-length GFP-tagged syntaxin 3 with the FMDE motif mutated to four alanines. OS, outer segment; IS, inner segment; N, outer nuclear layer; ST, synaptic terminal. Bars, 5 µm.

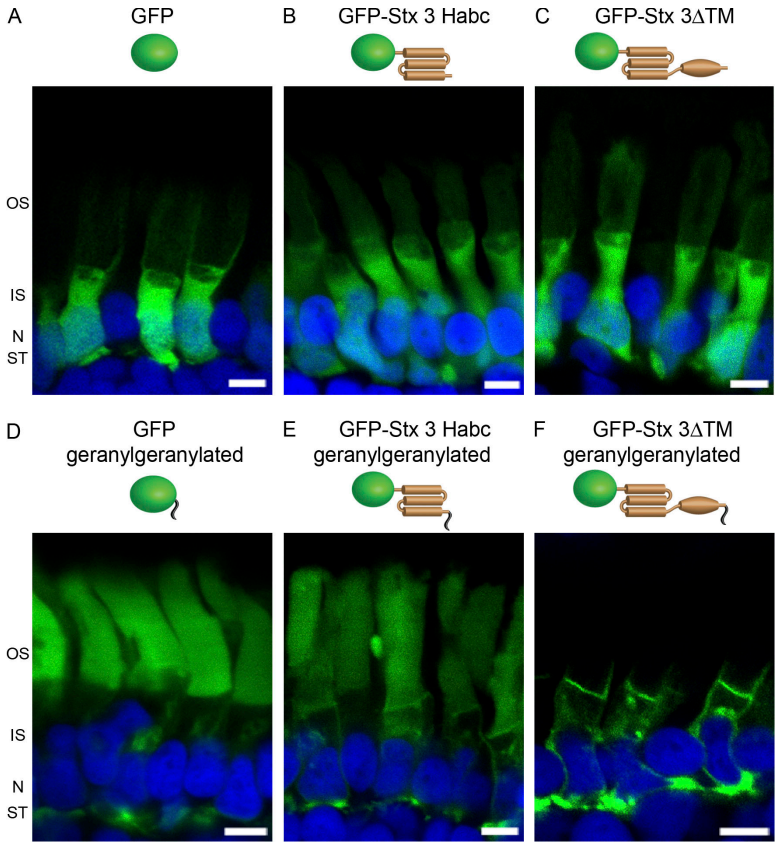

Figure 5. **Localization of soluble and geranylgeranylated GFP-tagged syntaxin 3 mutants in transgenic *Xenopus* rods.** (A) Soluble GFP. (B) GFP-tagged syntaxin 3 lacking both the SNARE and transmembrane domains. (C) GFP-tagged syntaxin 3 lacking the transmembrane domain. (D) Geranylgeranylated GFP. (E) Geranylgeranylated GFP-tagged syntaxin 3 lacking the SNARE homology domain and transmembrane domain. (F) Geranylgeranylated GFP-tagged syntaxin 3 lacking the transmembrane domain. OS, outer segment; IS, inner segment; N, outer nuclear layer; ST, synaptic terminal. Bars, 5 µm.

was found in internal membranes of the inner segment (Fig. 4 B). However, the deletion of the SNARE domain redirected a large portion of the expressed protein to the outer segment (Fig. 4 C), with an overall pattern mirroring that of R9AP. The deletion of the entire cytoplasmic domain of syntaxin 3, leaving just the transmembrane domain, also resulted in robust outer segment localization (Fig. 4 D). This analysis suggests that the intracellular targeting information for syntaxin 3 is coded within the SNARE domain.

We next tested whether the targeting role of the SNARE domain could be fully preserved when the adjacent transmembrane domain is removed. However, just deleting the transmembrane domain (or both SNARE and transmembrane domains) from GFP-tagged syntaxin 3 resulted in protein distributions similar to that of soluble GFP, which reflects the availability of the rod cytoplasm (Fig. 5, compare B and C to A; Knox et al., 1998; Peet et al., 2004). To make these constructs membrane associated we placed a CaaX box (CIIL) on the C termini of these proteins to enable their geranylgeranylation. This modification dramatically changed the intracellular localization of both constructs lacking the SNARE domain to the outer segment (Fig. 5, D and F), whereas the construct containing the SNARE domain was localized to the synaptic terminus and the plasma membrane of the inner segment (Fig. 5 E), just as the full-length syntaxin 3 in Fig. 4 A.

Together, the data from Figs. 4 and 5 indicate that the SNARE domain plays a decisive role in setting the subcellular localization of syntaxin 3. They further demonstrate that the removal of targeting information releases this protein primarily to the outer segment (as far as the resulting construct remains membrane associated). This suggests that the outer segment may serve as a default destination for membrane protein delivery in this cell type, a suggestion tested in the subsequent experiments.

It should be also noted that a study of syntaxin 3 in epithelial cells did not reveal that the SNARE domain was required for its normal subcellular localization to the apical rather than the basolateral plasma membrane and instead demonstrated that a four–amino acid FMDE motif within the Habc domain was required (Sharma et al., 2006). To determine if this motif plays any role in the localization of syntaxin 3 in photoreceptors, we replaced the FMDE sequence with four alanines and found that this mutation had no effect on syntaxin 3 targeting in rods (Fig. 4 E), illustrating that different cell types can use different information for targeting the same protein.

Subcellular targeting of R9AP/syntaxin 3 chimeras

An alternative approach we used to identify regions within the R9AP and syntaxin 3 molecules involved in their targeting was to analyze subcellular distributions of a series of chimeric constructs containing various combinations of domains from each of these two proteins (Fig. 6). Because of the propensity for several of the GFP-tagged chimeric molecules to form aggresomes (not depicted), we instead used the Myc-tagged versions of these constructs. Replacement of R9AP's transmembrane domain (sufficient for its primarily outer segment localization) with the one from syntaxin 3 had no effect on the chimera's

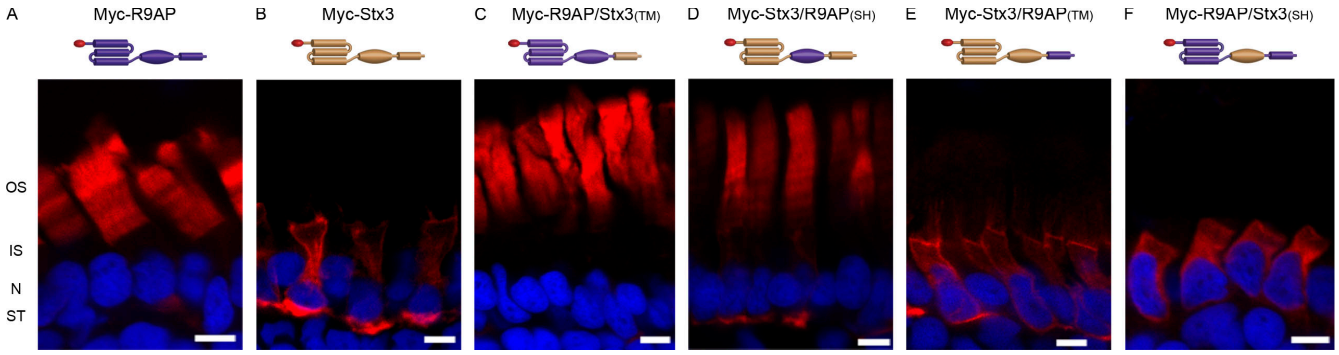

Figure 6. **Localization of Myc-tagged R9AP/syntaxin 3 chimeras in transgenic *Xenopus* rods.** (A) Full-length Myc-tagged R9AP. (B) Full-length Myc-tagged syntaxin 3 (Stx3). (C) Myc-tagged chimera of R9AP containing the transmembrane domain from Stx3. (D) Myc-tagged chimera of syntaxin 3 containing the SNARE homology domain from R9AP. (E) Myc-tagged chimera of syntaxin 3 containing the transmembrane domain from R9AP. (F) Myc-tagged chimera of R9AP containing the SNARE homology domain from syntaxin 3. OS, outer segment; IS, inner segment; N, outer nuclear layer; ST, synaptic terminal. Bars, 5 µm.

localization (Fig. 6, compare C to A), once again confirming that the transmembrane domain is not involved in syntaxin 3 targeting. However, the replacement of the SNARE homology domain of syntaxin 3 (sufficient for its exclusion from the outer segment) with the one from R9AP completely shifted the chimera's localization to the R9AP-like pattern (Fig. 6 D). The replacement of the transmembrane domain from syntaxin 3 with that of R9AP resulted in a molecule maintaining the syntaxin 3 localization pattern (Fig. 6, compare E to B). However, replacement of the SNARE homology domain from R9AP with that of syntaxin 3 prevented the molecule from targeting to the outer segments (Fig. 6 F). A detailed description of each chimeric molecule is provided in Table S1 (available at http://www.jcb.org/cgi/content/full/jcb.200806009/DC1).

Consistent with the results of the deletion mutagenesis, these data provide complementary evidence that the SNARE homology domain in syntaxin 3 plays an active role in excluding this protein from the outer segment. To the contrary, the transmembrane domain of R9AP does not appear to be unique in directing outer segment targeting. But are the transmembrane domains from R9AP and syntaxin 3 interchangeable because they belong to structurally related proteins or would any transmembrane domain lacking specific targeting information be targeted to the outer segment?

The length of a transmembrane domain is critical for outer segment targeting

To address this question, we analyzed the targeting of other GFP-tagged transmembrane domains from proteins either not expressed in photoreceptors or not present in the outer segments. For the former, we chose the first transmembrane segment of the metabotropic glutamate receptor 1 (mGluR1), which is not expressed in rods (Koulen et al., 1997; Sen and Gleason, 2006). As shown in Fig. 7, this "random" transmembrane construct accumulated in the outer segments, similarly to R9AP.

For the non-outer segment proteins, we choose microsomal cytochrome b5 and BclXL, an antiapoptotic protein that resides in the mitochondrial outer membrane. Like R9AP and syntaxin 3, these proteins contain a single pass transmembrane domain at their C termini. In the case of cytochrome b5 (Pedrazzini et al., 2000), the transmembrane domain is sufficient to ensure the localization of reporter molecules to the ER. This property is dictated by the relatively short length of the cytochrome b5 transmembrane domain, predicted to contain 14 amino acids (Table S2, available at http://www.jcb.org/cgi/content/full/jcb.200806009/DC1). Increasing this length by several hydrophobic amino acids shifts the intracellular localization from the ER to the plasma membrane in the fibroblast cell line CV-1 (Pedrazzini et al., 1996). The data from Fig. 8 A demonstrate that in *Xenopus* rods the construct containing a GFP-tagged cytochrome b5 transmembrane domain is targeted to internal membranes of the inner segment where it overlaps with the ER marker protein, calnexin (Fig. S2). However, increasing the length of this transmembrane domain by four amino acids redirected it almost exclusively to the outer segment (Fig. 8 B).

In the case of BclXL, its mitochondrial localization is determined by the positively charged residues in the sequence immediately flanking the transmembrane domain (Kaufmann et al., 2003). We confirmed that the corresponding GFP-tagged

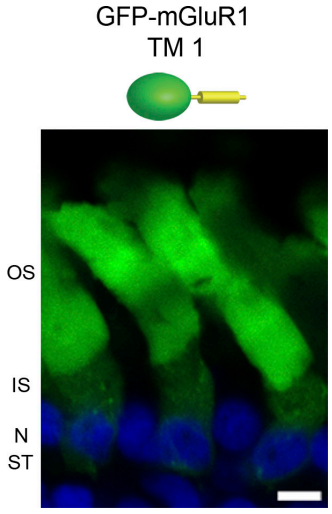

Figure 7. **Localization of a random GFP-tagged transmembrane domain in transgenic *Xenopus* rods.** GFP-tagged transmembrane segment 1 from mGluR1. Bar, 5 µm.

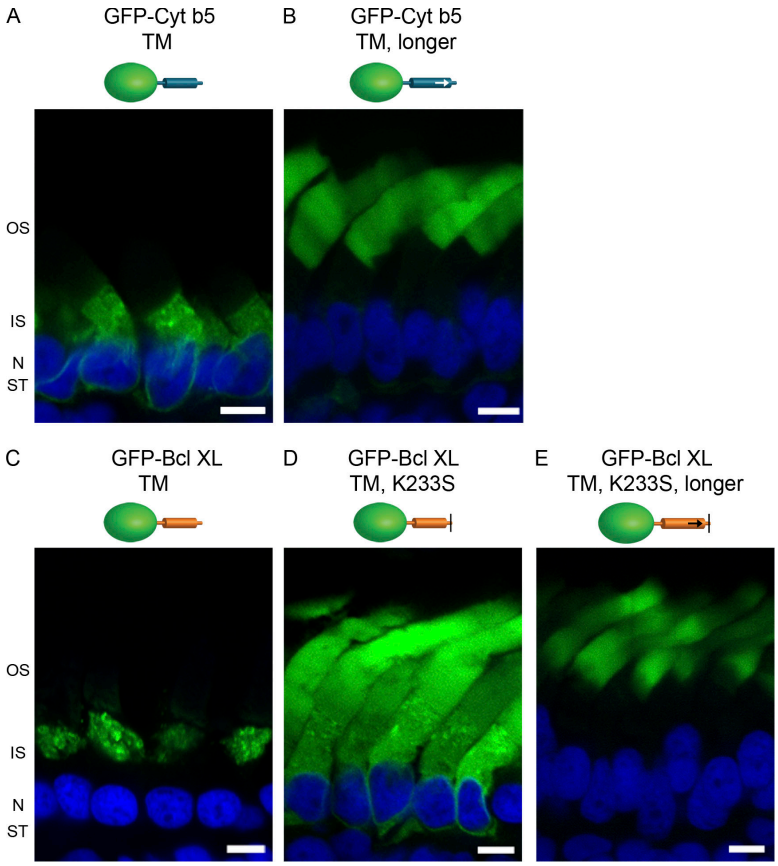

Figure 8. **Localization of ER and mitochondrial-targeted GFP-tagged transmembrane domains and their length mutants in transgenic *Xenopus* rods.** The following constructs were expressed as GFP fusion proteins in *Xenopus* rods (see Table S2 for sequence details, available at http://www.jcb.org/cgi/content/full/jcb.200806009/DC1): (A) transmembrane domain from microsomal cytochrome b5 (Cyt b5); (B) transmembrane domain from cytochrome b5 elongated by four amino acid residues; (C) transmembrane domain from Bcl XL; (D) transmembrane domain from Bcl XL bearing a point mutation (K233S); (E) transmembrane domain from Bcl XL bearing the K233S mutation and elongated by four amino acid residues. OS, outer segment; IS, inner segment; N, outer nuclear layer; ST, synaptic terminal. Bars, 5 µm.

construct correctly targets to the mitochondria in *Xenopus* rods (note that in photoreceptors the mitochondria cluster in the apical end of the inner segment; Fig. 8 C). The substitution of the critical C-terminal lysine (K233 in the full-length BclXL protein) for a serine released this construct to membranes throughout the rod cell (Fig. 8 D). This does not resemble the distribution of R9AP but we noticed that the predicted length of the mutant transmembrane domain is shorter than in R9AP, as in the case of cytochrome b5 (13 residues; Table S2). Therefore, we increased this length by four residues, and the resulting construct was overwhelmingly targeted to the outer segment (Fig. 8 E).

Conversely, when we decreased the length of the transmembrane domain of R9AP (predicted to contain 17 residues; Table S2) by either two or four residues, the localization of the resulting constructs gradually shifted from primarily outer segment to inner segment internal membranes (Fig. 9, A–C). Western blots of soluble versus membrane fractions from transgenic tadpole retinas were used to verify that the shortening of R9AP's transmembrane domain did not significantly change its membrane association (Fig. 9 D). Additionally, the transmembrane domain shortened by two residues was used to replace the normal transmembrane domain in full-length R9AP, which caused this molecule to shift localization from the outer segment to a mix of outer and inner segment internal membranes similar to the GFP molecule with this transmembrane domain (Fig. S3, available at http://www.jcb.org/cgi/content/full/jcb.200806009/DC1).

Collectively, our data from five different examples suggest that proteins containing transmembrane domains of sufficient length are predisposed to traffic to the outer segment, regardless of their specific amino acid composition.

Do proteins targeted by default to photoreceptor outer segments target to cilia in other cell types?

The rod outer segment is a modified primary cilium (for review see Besharse et al., 2003). Therefore, in the last set of control experiments, we tested whether the pattern of preferential membrane protein localization to the outer segment is a property of the photoreceptor cell or ciliary structures in general. We generated transgenic tadpoles expressing either GFP-tagged R9AP or the GFP-tagged transmembrane domain from syntaxin 3 (both targeted to rod outer segments by default) in a nontissue-specific manner under the control of a ubiquitous CMV promoter. In general, these reporters displayed essentially identical localization patterns throughout the tadpole body, although the latter construct had a much lower propensity to form aggresomes. Three examples are shown in Fig. 10. In photoreceptors, the CMV promoter drove expression in cones much more abundantly than in rods, providing us with a chance to show that both types of photoreceptors handle these proteins similarly by targeting them to the outer segments (Fig. 10 A). In the cells of the nasal pit, which at this developmental stage consists of both ciliated and nonciliated olfactory neurons and support cells (Hansen et al., 1998), the reporter proteins were found throughout the cell with the notable exception that they were absent from the cilia, visualized by labeling with acetylated α-tubulin (Fig. 10 B). The epidermis of the tadpole consists of mucous-secreting cells regularly interspaced with epidermal cells containing

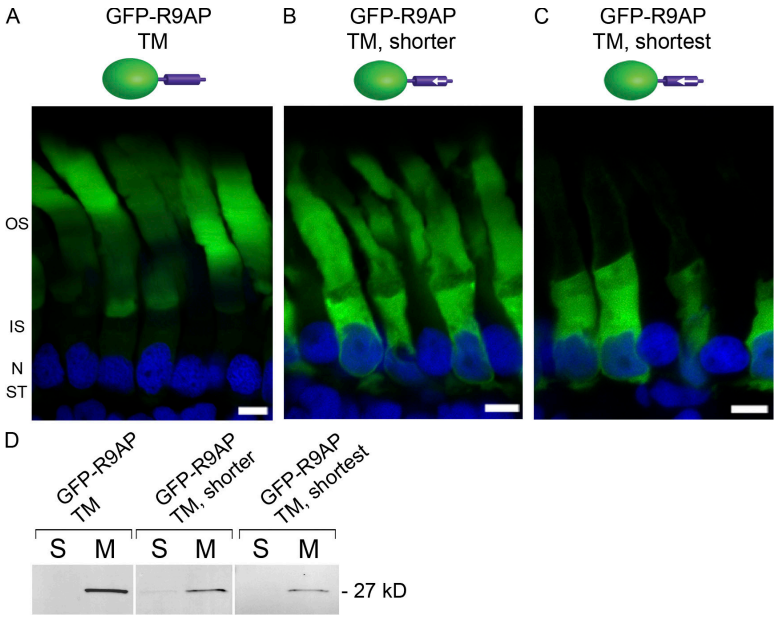

Figure 9. **Localization of GFP-tagged R9AP transmembrane domain length mutants in transgenic *Xenopus* rods.** (A) GFP-tagged transmembrane domain from R9AP. (B) GFP-tagged transmembrane domain from R9AP shortened by two amino acid residues. (C) GFP-tagged transmembrane domain from R9AP shortened by four amino acid residues. (D) *Xenopus* tadpole retinas expressing GFP-tagged R9AP transmembrane domains of various lengths as indicated were fractionated into soluble and membrane pools by sonication and sedimentation at 120,000 *g*. Proteins in each fraction were Western blotted using an antibody against GFP. Lane S, soluble protein fraction; lane M, membrane fraction. OS, outer segment; IS, inner segment; N, outer nuclear layer; ST, synaptic terminal. Bars, 5 µm.

multiple motile cilia (Steinman, 1968). In these cells, the reporter proteins were localized nonspecifically to the plasma membrane but were absent from the cilia (Fig. 10 C). Together, these data argue that the membrane protein trafficking pattern in rods and cones is not determined simply by the presence of a ciliary organelle.

Discussion

The compartmentalized organization of vertebrate photoreceptors is elegantly suited to serve their function as highly sensitive light detectors. Yet, little is known about the mechanisms targeting individual proteins to their respective intracellular compartments in these cells. Most recently, substantial effort has been directed toward studying proteins targeting to the outer segment, with a strong emphasis on the trafficking of rhodopsin. In this study, we took a more general look at this problem by comparing the targeting of two related proteins, syntaxin 3 and R9AP, into the two distinctly separate plasma membrane domains, the outer segment and the remainder of the cell. Our major finding is that, whereas specific targeting information was required for achieving protein localization outside the outer segment, no sequence-specific signals were required for the outer segment targeting as far as a protein contained a transmembrane domain of sufficient length and lacked overriding sequence signals targeting it elsewhere. This suggests that the outer segment protein composition could be achieved by having only one or a few proteins that actively direct vesicular trafficking to this compartment. Other membrane proteins, such as R9AP, may potentially be cotransported in the same vesicles. Here we will discuss how this idea fits the current understanding of photoreceptor outer segment trafficking.

Outer segment protein targeting in photoreceptors

Membrane protein trafficking to the outer segment has been studied most extensively for rhodopsin and is thought to consist of several discrete steps (for reviews see Papermaster, 2002; Williams, 2004; Deretic, 2006). After synthesis at the ER and passing through the Golgi, rhodopsin is sorted into newly budding vesicular transport carriers. This is mediated by the interaction between the VXPX targeting sequence in rhodopsin's C terminus (Deretic et al., 1998; Tam et al., 2000) and the small GTP binding protein ARF4 (Deretic et al., 2005). Other small GTP binding proteins, rab6 and rab11, also play a role in formation of the rhodopsin carriers in the trans-Golgi (for review see Deretic, 2006). The carriers are then delivered to the base of the cilium connecting the inner and outer segments with the aid of the motor cytoplasmic dynein (Tai et al., 1999). There the carriers dock and fuse with a specialized region of the plasma membrane separated from the plasma membrane of the inner segment via a diffusional barrier. This docking is assisted by another set of small GTP binding proteins, rac1 and rab8 (Moritz et al., 2001a; Deretic et al., 2004). Rhodopsin then moves laterally through the membrane of the connecting cilium into the outer segment, possibly assisted by cytoskeletal motors (Liu et al., 1999; Marszalek et al., 2000). The V(I)XPX signal is also present in cone opsins and in photoreceptor-specific retinol dehydrogenase (Deretic et al., 1998; Tam et al., 2000; Luo et al., 2004) but not in any other proteins resident in the outer segment.

This major transport pathway is necessary for the outer segment to form and for the cell to survive. For example, the lack of outer segment formation and severe degeneration observed in rhodopsin knockout mice (Humphries et al., 1997; Lem et al., 1999) can be rescued by the expression of normal rod or cone opsin (Concepcion et al., 2002; Guang Shi, 2004), but not by rhodopsin in which the VXPX sequence has been deleted (Concepcion et al., 2002; Lee and Flannery, 2007). However, when rhodopsin lacking the VXPX sequence is expressed in rods in addition to normal rhodopsin, outer segments are formed with most mutant molecules observed inside the outer segment and a smaller fraction in other cellular compartments,

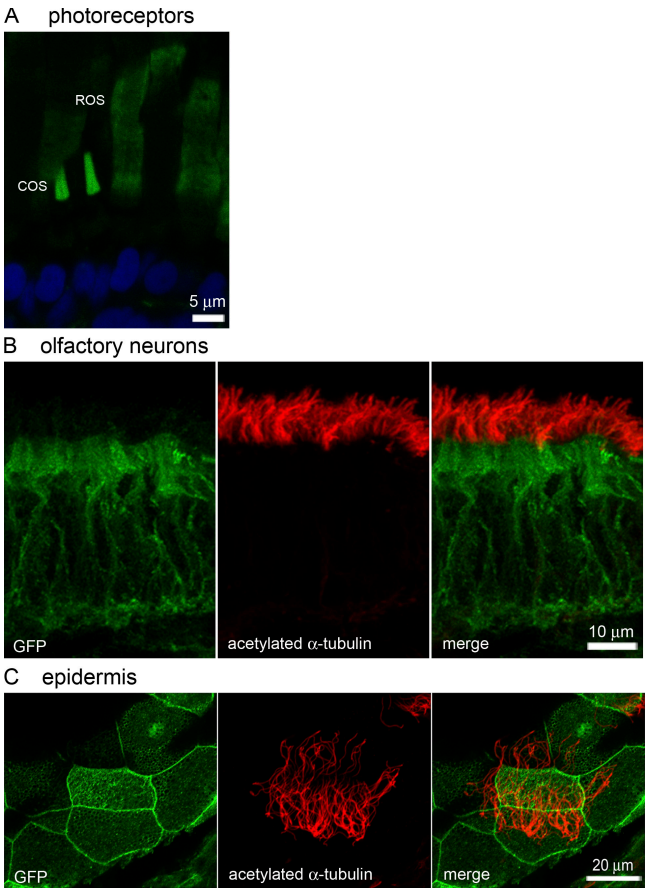

Figure 10. **Patterns of transgenic GFP-R9AP or GFP-syntaxin 3 transmembrane domain expression in ciliated *Xenopus* tissues.** (A) GFP-tagged full-length R9AP expressed in photoreceptors. (B) GFP-tagged transmembrane domain from syntaxin 3 expressed in olfactory cells and in the epidermis (C). (B and C) Cilia are labeled with an antibody against acetylated α-tubulin (red). COS, cone outer segment; ROS, rod outer segment.

resembling the normal R9AP distribution (Sung et al., 1994; Li et al., 1996; Green et al., 2000; Moritz et al., 2001b; Concepcion et al., 2002; Kraft et al., 2005; Tam et al., 2006; Lee and Flannery, 2007). The V(I)XPX-dependent pathway may not be the only one targeting proteins to the outer segment because peripherin 2 has an alternative targeting sequence, and it has been suggested that delivery of this protein relies on a distinct set of transport vesicles (Fariss et al., 1997; Tam et al., 2004; Lee et al., 2006). Most recently, it has been speculated that guanylate cyclase is another protein that marks independent carriers to the outer segment, yet no details of how these putative vesicles are assembled and targeted are known (Karan et al., 2007).

Outer segment protein localization can be achieved without specific targeting signals

Here we have shown that a key signaling protein, R9AP, can be delivered to the outer segment without containing any specific targeting signals coded in its sequence. Furthermore, every other transmembrane protein construct that we tested was delivered to the rod outer segment as far as it obeyed two simple rules. First, the transmembrane domain had to be of a sufficient length. This most likely reflects the phenomenon of hydrophobic matching whereby short transmembrane domains partition into the thin bilayer of the ER and the longer transmembrane domains preferentially partition into the thicker bilayers of the Golgi and post-Golgi components of the secretory pathway, which contain more sterols and complex sphingolipids (for review see Killian, 1998; Andersen and Koeppe, 2007; van Meer et al., 2008). Second, the protein had to be stripped of any targeting information directing it to other subcellular compartments.

The first rule was established by showing that increasing the length of cytochrome b5's transmembrane domain redirected it from the ER to the outer segment and, conversely, the reduction in the length of R9AP's transmembrane domain had the opposite effect of shifting its localization from primarily outer segments to ER. The second rule was demonstrated with syntaxin 3, which was redirected from the plasma membrane of the inner segment and synaptic terminal to the outer segment upon the loss of its SNARE homology domain. BclXL bridged both rules: its redirection from mitochondria to outer segments required both an increase in the length of the transmembrane domain and a reduction in the positive charge in the flanking region. Finally, a randomly selected transmembrane segment from metabotropic glutamate receptor 1, which obeyed both rules, localized predominantly to the outer segment.

Interestingly, the ability of the SNARE domain of syntaxin 3 to mediate exclusion from the outer segment was retained when the transmembrane domain was replaced by geranylgeranylation. Intracellular localization of a protein containing the SNARE domain of syntaxin 3 was indistinguishable from normal syntaxin 3, whereas protein constructs lacking this targeting domain were localized predominantly to the outer segment, similar to transmembrane domain containing proteins carried by the default pathway. This is consistent with previous results that GFP-tagged constructs that were myristoylated or palmitoylated predominantly localized to the outer segment as well (Tam et al., 2000). It is intriguing to speculate that peripheral membrane proteins may use the same default targeting pathway as the proteins we analyzed in this study. However, in the absence of a systematic analysis this idea should be treated cautiously particularly because all cells, including photoreceptors, express an array of proteins specifically binding to lipidated proteins and regulating their intracellular localization. Examples of such proteins actively studied in photoreceptors include the prenyl binding protein PrBP/δ, which regulates the outer segment localization of rhodopsin kinase and the cyclic guanosine monophosphate phosphodiesterase (Norton et al., 2005; Zhang et al., 2007), and phosducin, which regulates the inner–outer segment translocation of the transducin βγ subunit (Sokolov et al., 2004).

Notably, we have also found that the targeting information of syntaxin 3 in photoreceptors is coded differently than in epithelial cells, where its normal localization in the apical plasma membrane is determined by the FMDE motif (Sharma et al., 2006). Substitutions of these amino acids in epithelial cells caused a randomized syntaxin 3 distribution throughout both apical and basolateral membranes. However, the substitution of the entire motif with alanines in transgenic frog rods did not affect its normal inner segment plasma membrane distribution. This example illustrates that different cell types may use different mechanisms for achieving specific intracellular targeting.

The actual mechanism by which the SNARE domain directs syntaxin 3 targeting in rods remains beyond the scope of this study. Because the SNARE domain is the region involved in almost all known protein–protein interactions, there are several possibilities including that this domain encodes a specific signal (interacting with a component of vesicular trafficking such as a Rab GTPase or coat protein), which could be conformation dependent (Mancias and Goldberg, 2007), or that syntaxin 3 must assemble into a SNARE protein complex, which again could either reveal a conformation-dependent targeting signal or provide an interaction partner that binds directly to a component of the vesicular trafficking machinery (Mossessova et al., 2003).

In summary, our findings indicate that the default route of membrane protein trafficking in photoreceptors is directed to the outer segment. This mode of delivery is so reliable that it is used for trafficking R9AP, a protein whose expression level is tightly regulated in photoreceptors and sets the dominant rate constant at which the cell recovers from the photoresponse (Krispel et al., 2006). This raises important questions concerning the interplay between targeted and default protein flow in these cells.

The relation between default and targeted protein trafficking in photoreceptors

Essential to understanding default trafficking patterns mechanistically is the recognition that intracellular vesicular transport always requires at least one cargo protein to contain specific signals that regulate their delivery to individual subcellular locations (for reviews see Muth and Caplan, 2003; Rodriguez-Boulan and Musch, 2005). This suggests that proteins lacking such signals and carried by default pathways have to be copackaged into the same vesicles as proteins that do carry specific targeting information. Therefore a straightforward hypothesis to explain the outer segment delivery of R9AP is that it is transported in the same post-Golgi vesicles as rhodopsin, the most abundant transport vesicles in this cell. In this case, even a random incorporation of proteins lacking a targeting signal into all types of transport carrier vesicles would result in the majority reaching the outer segment and only a small fraction delivered elsewhere. Consistently, a small fraction of R9AP is always found outside the outer segment (Hu and Wensel, 2002; Martemyanov et al., 2003; this study). Similarly, when rhodopsin mutants lacking the VXPX sequence are expressed in rods containing normal rhodopsin, they display a localization pattern very similar to that of R9AP, with the majority found in the outer segment and a minor fraction in the inner segment membranes (compare Fig. 6 from Moritz et al. [2001b] with Fig. 2). This was interpreted as the mutant rhodopsin cotransporting with the wild-type rhodopsin (Concepcion et al., 2002). The new development in this study is that such cotransport may serve as the normal route of outer segment delivery for a functional protein, R9AP.

The next interesting consideration is whether the incorporation of proteins lacking a targeting signal into all types of transport carrier vesicles is random or if it is possible that vesicles carrying proteins to destinations other than the outer segment are less permissive for random protein incorporation than those responsible for the default trafficking flow. Additionally, the degree of this permissiveness may be affected by the specific properties of individual proteins. Indeed, for the various protein constructs using the default pathway, we observed a significant variation in the amounts present outside the outer segment (including an apparent lack for mutated BclXl or cytochrome b5). Although some of this variation may relate to the differences in the constructs' expression levels, it could also reflect the relative permissiveness of different types of transport vesicles to incorporate individual proteins. Addressing these questions requires identification of all the major classes of transport carriers in photoreceptors, which is an exciting direction of future studies.

Importantly, the default mode of protein delivery can be used only on the condition that minor mislocalization is not harmful for the cell. Accordingly, the overexpression of the proteins using the default trafficking flow that we examined here did not cause any overt signs of photoreceptor stress or lead to death in the time frame of this study. Furthermore, the normal "leak" of R9AP appears nonconsequential. This is in contrast to rhodopsin, where even minor mislocalization leads to photoreceptor degeneration, although not nearly as severe as in the absence of normal rhodopsin (Lee and Flannery, 2007).

Another logical question is whether other integral or even peripheral membrane proteins use the default trafficking pathway in photoreceptors. This is an exciting topic to explore, particularly given that nearly nothing is known about the delivery of many proteins responsible for signaling and maintenance in the outer segment (such as guanylate cyclase, ABCR transporter, or cyclic guanosine monophosphate–gated channel, just to mention a few). But perhaps an even more significant consequence of our finding that the default protein flow in photoreceptors is directed to outer segments is the implication that every membrane protein residing in other cellular compartments has to use specific mechanisms to avoid this destination. Disruption of the targeting information in each non-outer segment protein did not simply yield a randomized distribution among all cellular membranes, but resulted in substantial redirection to the outer segment. This calls for expanding the questions in addressing protein targeting in photoreceptors from what allows a restricted subset of cellular proteins to reach the outer segment to what allows the greater number of membrane proteins residing in other cellular compartments to avoid the outer segment.

Lastly, it is interesting to consider the possibility that other differentiated cells may use an interplay between specific targeting mechanisms and default trafficking patterns to meet their compartmentalization needs. Traditionally, a constitutive (or default) trafficking pathway was considered to account for the bulk of protein trafficking to the plasma membrane, at least in nonpolarized cells (for review see Ponnambalam and Baldwin, 2003). Polarized cells are more complex and many proteins that were initially thought to be delivered by default have now been shown to be delivered in a signal-dependent manner (for review see Rodriguez-Boulan and Musch, 2005). Our findings in photoreceptors indicate that default trafficking may be reliable enough for the delivery of a key signaling protein, which may call for reconsidering the relative contributions of default and targeted trafficking in various cells. However, the example of photoreceptors also illustrates that this should be explored in the context of each specific cell type.

Materials and methods

Generation of transgenic tadpoles

Transgenic *Xenopus* tadpoles were produced using restriction enzyme–mediated integration developed previously (Kroll and Amaya, 1996; Amaya and Kroll, 1999) with modifications (described in Batni et al., 2000; Whitaker and Knox, 2004). A minimum of four individual transgenic animals were evaluated for every DNA construct.

The constructs were generated using standard PCR-based subcloning methods. Fusion constructs and large deletions were generated using splicing by overhang extension PCR primers; point mutations and small deletions or insertions were generated using the QuikChange II XL kit (Stratagene). PCR products were subcloned into the XOP5.5 vector (Knox et al., 1998) and confirmed by direct sequencing. DNA templates were obtained as follows: IMAGE clones corresponding to *Xenopus* R9AP1, R9AP2, and syntaxin 3 were purchased from American Type Culture Collection; portions of cytochrome b5, Bcl-XL, and mGluR1 were amplified from a mouse brain cDNA library (Stratagene); the Myc epitope was constructed from the pCMV-Myc vector (BD Biosciences); the CMV promoter was subcloned from the CS2p+ vector (a gift from D. Turner, University of Michigan, Ann Arbor, MI).

To facilitate identification of transgenic animals expressing Myc-tagged proteins we took advantage of the dual promoter strategy described in Fu et al. (2002). In addition to the *Xenopus* opsin promoter driving expression of the various Myc-tagged constructs in rods, we added a cassette containing the γ-crystallin promoter driving GFP expression in the lens. This reporter cassette was subcloned from pDPCG (a gift from Y.-B. Shi, National Institutes of Health, Bethesda, MD).

Histology

Transgenic tadpoles at development stages 43–54 were fixed in 4% paraformaldehyde, cryoprotected in 30% sucrose, and frozen in 100% tissue-freezing medium. In all animals expressing GFP fusion constructs, tissue sections were stained with 2 µg/ml Hoechst 33342 (Invitrogen) to label the nuclei and analyzed using a microscope (Eclipse 90i; Nikon) with a Plan Apo VC 100×, 1.4 NA oil immersion lens (Nikon), and a C1 confocal scanner controlled by EZ-C1 v 3.10 software (Nikon). Manipulation of images was limited to adjusting the brightness level, image size, and cropping using either EZ-C1 v 3.10 Viewer or Photoshop (Adobe). To detect Myc-tagged constructs, tissue sections were permeabilized with 0.5% Triton X-100, blocked with 5% normal goat serum, incubated with a mouse monoclonal anti-Myc antibody (9E10; Santa Cruz Biotechnology, Inc.), rinsed in PBS Tween 20, and incubated with anti–mouse IgG secondary antibodies conjugated to Alexa Fluor 594 (Invitrogen) and Hoechst 33342. Phalloidin conjugated to Alexa fluor 594 (Invitrogen) as a label of F-actin was used to mark calycal processes. For analysis of the nasal pit and epidermis, intact animals were fixed in 4% paraformaldehyde, incubated with mouse antiacetylated tubulin clone 6-11B-1 (Sigma-Aldrich) in blocker containing 0.5% Triton X-100 and 5% normal goat serum overnight at 4°C, and washed and incubated in anti–mouse IgG secondary antibodies conjugated to Alexa Fluor 594 for 4 h at room temperature. The animals were then embedded in 4% agarose and 50–100-µm sections were cut on a vibrotome and collected directly onto slides. Additional antibodies included affinity purified rabbit polyclonal antibody against GST-xR9AP2 fragment (residues 1–239), affinity purified rabbit anti-peptide antibody against residues 103–114 of xR9AP1, rabbit anti–syntaxin 3 (Abcam), and rabbit anti-GFP A.v. peptide (Clontech Laboratories, Inc.).

RT-PCR

RNA was extracted from adult *Xenopus* retina using the RNeasy Mini kit (QIAGEN) and treated with DNase I. SuperScript III reverse transcriptase (Invitrogen) and gene-specific primers were used to generate cDNA from 50 ng RNA. Amplification of the cDNA was performed using a standard PCR cycle and Taq DNA polymerase, and products were analyzed on an ethidium bromide–stained agarose gel.

Protein and membrane preparations

Recombinant protein standards consisting of GST fused to the cytoplasmic domains of xR9AP1 or xR9AP2 were expressed in Arctic Express (DE3) RIL cells (Stratagene) and purified on glutathione sepharose beads as previously described (Baker et al., 2006). Membrane fractions of *Xenopus* retina were prepared by sonication in PBS followed by ultracentrifugation in an Airfuge (Beckman Coulter) at 100,000 *g* for 15 min. Preparative immunoprecipitation of RGS9 performed using the sheep antibody against the C terminus of bovine RGS9 and the subsequent identification of coprecipitating proteins was performed by Western blotting and mass spectrometry as described in Martemyanov et al. (2005). Isolated frog rod outer/inner segment fragments were obtained from a wild-type tadpole by gentle agitation of the retina in frog Ringer's solution (115 mM NaCl, 2 mM KCl, 1 mM $CaCl_2$, 1 mM $MgCl_2$, and 5 mM Hepes, pH 7.4). The fragments were allowed to settle onto a concavalin A (Sigma-Aldrich)–coated glass slide and immunostained as described in the Histology section.

Online supplemental material

Fig. S1 shows the localization of Myc-tagged R9AP and two Myc-tagged R9AP deletion constructs to the outer segments of transgenic tadpole photoreceptors. Fig. S2 shows colocalization of the expressed GFP-tagged cytochrome b5 transmembrane domain with the ER marker calnexin. Fig. S3 shows the localization of a Myc-tagged R9AP variant with a shortened transmembrane domain in transgenic tadpole photoreceptors. Table S1 describes the exact breakpoints of the R9AP/syntaxin 3 chimeric molecules presented in Fig. 6. Table S2 describes the sequence and length of the GFP-tagged transmembrane domains used in this study. Online supplemental material is available at http://www.jcb.org/cgi/content/full/jcb.200806009/DC1.

We thank Enrique Rodriguez-Boulan, Joseph Besharse, and Kirill Martemyanov for critically reading the manuscript.

This work was supported by grants from the National Institutes of Health (EY12859 to V.Y. Arshavsky and EY12975 to B.E. Knox) and by a Core Grant for Vision Research to Duke University (EY5722).

Submitted: 2 June 2008
Accepted: 6 October 2008

References

Amaya, E., and K.L. Kroll. 1999. A method for generating transgenic frog embryos. *Methods Mol. Biol.* 97:393–414.

Andersen, O.S., and R.E. Koeppe II. 2007. Bilayer thickness and membrane protein function: an energetic perspective. *Annu. Rev. Biophys. Biomol. Struct.* 36:107–130.

Baker, S.A., K.A. Martemyanov, A.S. Shavkunov, and V.Y. Arshavsky. 2006. Kinetic mechanism of RGS9-1 potentiation by R9AP. *Biochemistry.* 45:10690–10697.

Batni, S., S.S. Mani, C. Schlueter, M. Ji, and B.E. Knox. 2000. *Xenopus* rod photoreceptor: model for expression of retinal genes. *Methods Enzymol.* 316:50–64.

Besharse, J.C., S.A. Baker, K. Luby-Phelps, and G.J. Pazour. 2003. Photoreceptor intersegmental transport and retinal degeneration: a conserved pathway common to motile and sensory cilia. *Adv. Exp. Med. Biol.* 533:157–164.

Chuang, J.Z., Y. Zhao, and C.H. Sung. 2007. SARA-regulated vesicular targeting underlies formation of the light-sensing organelle in mammalian rods. *Cell.* 130:535–547.

Concepcion, F., A. Mendez, and J. Chen. 2002. The carboxyl-terminal domain is essential for rhodopsin transport in rod photoreceptors. *Vision Res.* 42:417–426.

Deretic, D. 2006. A role for rhodopsin in a signal transduction cascade that regulates membrane trafficking and photoreceptor polarity. *Vision Res.* 46:4427–4433.

Deretic, D., S. Schmerl, P.A. Hargrave, A. Arendt, and J.H. McDowell. 1998. Regulation of sorting and post-Golgi trafficking of rhodopsin by its C-terminal sequence QVS(A)PA. *Proc. Natl. Acad. Sci. USA.* 95:10620–10625.

Deretic, D., V. Traverso, N. Parkins, F. Jackson, E.B. Rodriguez de Turco, and N. Ransom. 2004. Phosphoinositides, ezrin/moesin, and rac1 regulate fusion of rhodopsin transport carriers in retinal photoreceptors. *Mol. Biol. Cell.* 15:359–370.

Deretic, D., A.H. Williams, N. Ransom, V. Morel, P.A. Hargrave, and A. Arendt. 2005. Rhodopsin C terminus, the site of mutations causing retinal disease, regulates trafficking by binding to ADP-ribosylation factor 4 (ARF4). *Proc. Natl. Acad. Sci. USA.* 102:3301–3306.

Fariss, R.N., R.S. Molday, S.K. Fisher, and B. Matsumoto. 1997. Evidence from normal and degenerating photoreceptors that two outer segment integral membrane proteins have separate transport pathways. *J. Comp. Neurol.* 387:148–156.

Fu, L., D. Buchholz, and Y.B. Shi. 2002. Novel double promoter approach for identification of transgenic animals: a tool for in vivo analysis of gene function and development of gene-based therapies. *Mol. Reprod. Dev.* 62:470–476.

Green, E.S., M.D. Menz, M.M. LaVail, and J.G. Flannery. 2000. Characterization of rhodopsin mis-sorting and constitutive activation in a transgenic rat model of retinitis pigmentosa. *Invest. Ophthalmol. Vis. Sci.* 41:1546–1553.

Guang Shi, F.A.C., J. Chen. 2004. Targeting of visual pigments to rod outer segment in rhodopsin knockout mice. *In* Photoreceptor Cell Biology and Inherited Retinal Degenerations, vol. 10. D.S. Williams, editor. World Scientific Publishing Co. Pte. Ltd., River Edge, NJ. 93–1017.

Hansen, A., J.O. Reiss, C.L. Gentry, and G.D. Burd. 1998. Ultrastructure of the olfactory organ in the clawed frog, *Xenopus laevis*, during larval development and metamorphosis. *J. Comp. Neurol.* 398:273–288.

Hay, J.C. 2001. SNARE complex structure and function. *Exp. Cell Res.* 271:10–21.

Hu, G., and T.G. Wensel. 2002. R9AP, a membrane anchor for the photoreceptor GTPase accelerating protein, RGS9-1. *Proc. Natl. Acad. Sci. USA.* 99:9755–9760.

Humphries, M.M., D. Rancourt, G.J. Farrar, P. Kenna, M. Hazel, R.A. Bush, P.A. Sieving, D.M. Sheils, N. McNally, P. Creighton, et al. 1997. Retinopathy induced in mice by targeted disruption of the rhodopsin gene. *Nat. Genet.* 15:216–219.

Kaplan, M.W., R.T. Iwata, and R.C. Sears. 1987. Lengths of immunolabeled ciliary microtubules in frog photoreceptor outer segments. *Exp. Eye Res.* 44:623–632.

Karan, S., H. Zhang, S. Li, J.M. Frederick, and W. Baehr. 2007. A model for transport of membrane-associated phototransduction polypeptides in rod and cone photoreceptor inner segments. *Vision Res.* 48:442–452.

Kaufmann, T., S. Schlipf, J. Sanz, K. Neubert, R. Stein, and C. Borner. 2003. Characterization of the signal that directs Bcl-x_L, but not Bcl-2, to the mitochondrial outer membrane. *J. Cell Biol.* 160:53–64.

Keresztes, G., H. Mutai, H. Hibino, A.J. Hudspeth, and S. Heller. 2003. Expression patterns of the RGS9-1 anchoring protein R9AP in the chicken and mouse suggest multiple roles in the nervous system. *Mol. Cell. Neurosci.* 24:687–695.

Killian, J.A. 1998. Hydrophobic mismatch between proteins and lipids in membranes. *Biochim. Biophys. Acta.* 1376:401–415.

Knox, B.E., C. Schlueter, B.M. Sanger, C.B. Green, and J.C. Besharse. 1998. Transgene expression in *Xenopus* rods. *FEBS Lett.* 423:117–121.

Koulen, P., R. Kuhn, H. Wassle, and J.H. Brandstatter. 1997. Group I metabotropic glutamate receptors mGluR1alpha and mGluR5a: localization in both synaptic layers of the rat retina. *J. Neurosci.* 17:2200–2211.

Kraft, T.W., D. Allen, R.M. Petters, Y. Hao, Y.W. Peng, and F. Wong. 2005. Altered light responses of single rod photoreceptors in transgenic pigs expressing P347L or P347S rhodopsin. *Mol. Vis.* 11:1246–1256.

Krispel, C.M., D. Chen, N. Melling, Y.J. Chen, K.A. Martemyanov, N. Quillinan, V.Y. Arshavsky, T.G. Wensel, C.K. Chen, and M.E. Burns. 2006. RGS expression rate-limits recovery of rod photoresponses. *Neuron.* 51:409–416.

Kroll, K.L., and E. Amaya. 1996. Transgenic *Xenopus* embryos from sperm nuclear transplantations reveal FGF signaling requirements during gastrulation. *Development.* 122:3173–3183.

Lee, E.S., and J.G. Flannery. 2007. Transport of truncated rhodopsin and its effects on rod function and degeneration. *Invest. Ophthalmol. Vis. Sci.* 48:2868–2876.

Lee, E.S., B. Burnside, and J.G. Flannery. 2006. Characterization of peripherin/rds and rom-1 transport in rod photoreceptors of transgenic and knockout animals. *Invest. Ophthalmol. Vis. Sci.* 47:2150–2160.

Lem, J., N.V. Krasnoperova, P.D. Calvert, B. Kosaras, D.A. Cameron, M. Nicolo, C.L. Makino, and R.L. Sidman. 1999. Morphological, physiological, and biochemical changes in rhodopsin knockout mice. *Proc. Natl. Acad. Sci. USA.* 96:736–741.

Li, T., W.K. Snyder, J.E. Olsson, and T.P. Dryja. 1996. Transgenic mice carrying the dominant rhodopsin mutation P347S: evidence for defective vectorial transport of rhodopsin to the outer segments. *Proc. Natl. Acad. Sci. USA.* 93:14176–14181.

Liu, X., I.P. Udovichenko, S.D. Brown, K.P. Steel, and D.S. Williams. 1999. Myosin VIIa participates in opsin transport through the photoreceptor cilium. *J. Neurosci.* 19:6267–6274.

Luo, W., N. Marsh-Armstrong, A. Rattner, and J. Nathans. 2004. An outer segment localization signal at the C terminus of the photoreceptor-specific retinol dehydrogenase. *J. Neurosci.* 24:2623–2632.

Mancias, J.D., and J. Goldberg. 2007. The transport signal on Sec22 for packaging into COPII-coated vesicles is a conformational epitope. *Mol. Cell.* 26:403–414.

Marszalek, J.R., X. Liu, E.A. Roberts, D. Chui, J.D. Marth, D.S. Williams, and L.S. Goldstein. 2000. Genetic evidence for selective transport of opsin and arrestin by kinesin-II in mammalian photoreceptors. *Cell.* 102:175–187.

Martemyanov, K.A., P.V. Lishko, N. Calero, G. Keresztes, M. Sokolov, K.J. Strissel, I.B. Leskov, J.A. Hopp, A.V. Kolesnikov, C.K. Chen, et al. 2003. The DEP domain determines subcellular targeting of the GTPase activating protein RGS9 in vivo. *J. Neurosci.* 23:10175–10181.

Martemyanov, K.A., P.J. Yoo, N.P. Skiba, and V.Y. Arshavsky. 2005. R7BP, a novel neuronal protein interacting with RGS proteins of the R7 family. *J. Biol. Chem.* 280:5133–5136.

Morgans, C.W., J.H. Brandstatter, J. Kellerman, H. Betz, and H. Wassle. 1996. A SNARE complex containing syntaxin 3 is present in ribbon synapses of the retina. *J. Neurosci.* 16:6713–6721.

Moritz, O.L., B.M. Tam, L.L. Hurd, J. Peranen, D. Deretic, and D.S. Papermaster. 2001a. Mutant rab8 impairs docking and fusion of rhodopsin-bearing post-Golgi membranes and causes cell death of transgenic *Xenopus* rods. *Mol. Biol. Cell.* 12:2341–2351.

Moritz, O.L., B.M. Tam, D.S. Papermaster, and T. Nakayama. 2001b. A functional rhodopsin-green fluorescent protein fusion protein localizes correctly in transgenic *Xenopus laevis* retinal rods and is expressed in a time-dependent pattern. *J. Biol. Chem.* 276:28242–28251.

Mossessova, E., L.C. Bickford, and J. Goldberg. 2003. SNARE selectivity of the COPII coat. *Cell.* 114:483–495.

Mostov, K., T. Su, and M. ter Beest. 2003. Polarized epithelial membrane traffic: conservation and plasticity. *Nat. Cell Biol.* 5:287–293.

Muth, T.R., and M.J. Caplan. 2003. Transport protein trafficking in polarized cells. *Annu. Rev. Cell Dev. Biol.* 19:333–366.

Norton, A.W., S. Hosier, J.M. Terew, N. Li, A. Dhingra, N. Vardi, W. Baehr, and R.H. Cote. 2005. Evaluation of the 17-kDa prenyl-binding protein as a regulatory protein for phototransduction in retinal photoreceptors. *J. Biol. Chem.* 280:1248–1256.

Papermaster, D.S. 2002. The birth and death of photoreceptors: the Friedenwald Lecture. *Invest. Ophthalmol. Vis. Sci.* 43:1300–1309.

Pedrazzini, E., A. Villa, and N. Borgese. 1996. A mutant cytochrome b5 with a lengthened membrane anchor escapes from the endoplasmic reticulum and reaches the plasma membrane. *Proc. Natl. Acad. Sci. USA.* 93:4207–4212.

Pedrazzini, E., A. Villa, R. Longhi, A. Bulbarelli, and N. Borgese. 2000. Mechanism of residence of cytochrome b(5), a tail-anchored protein, in the endoplasmic reticulum. *J. Cell Biol.* 148:899–914.

Peet, J.A., A. Bragin, P.D. Calvert, S.S. Nikonov, S. Mani, X. Zhao, J.C. Besharse, E.A. Pierce, B.E. Knox, and E.N. Pugh Jr. 2004. Quantification of the cytoplasmic spaces of living cells with EGFP reveals arrestin-EGFP to be in disequilibrium in dark adapted rod photoreceptors. *J. Cell Sci.* 117:3049–3059.

Ponnambalam, S., and S.A. Baldwin. 2003. Constitutive protein secretion from the trans-Golgi network to the plasma membrane. *Mol. Membr. Biol.* 20:129–139.

Rodriguez-Boulan, E., and A. Musch. 2005. Protein sorting in the Golgi complex: shifting paradigms. *Biochim. Biophys. Acta.* 1744:455–464.

Sen, M., and E. Gleason. 2006. Immunolocalization of metabotropic glutamate receptors 1 and 5 in the synaptic layers of the chicken retina. *Vis. Neurosci.* 23:221–231.

Sharma, N., S.H. Low, S. Misra, B. Pallavi, and T. Weimbs. 2006. Apical targeting of syntaxin 3 is essential for epithelial cell polarity. *J. Cell Biol.* 173:937–948.

Sherry, D.M., R. Mitchell, K.M. Standifer, and B. du Plessis. 2006. Distribution of plasma membrane-associated syntaxins 1 through 4 indicates distinct trafficking functions in the synaptic layers of the mouse retina. *BMC Neurosci.* 7:54.

Sokolov, M., K.J. Strissel, I.B. Leskov, N.A. Michaud, V.I. Govardovskii, and V.Y. Arshavsky. 2004. Phosducin facilitates light-driven transducin translocation in rod photoreceptors. Evidence from the phosducin knockout mouse. *J. Biol. Chem.* 279:19149–19156.

Steinberg, R.H., S.K. Fisher, and D.H. Anderson. 1980. Disc morphogenesis in vertebrate photoreceptors. *J. Comp. Neurol.* 190:501–508.

Steinman, R.M. 1968. An electron microscopic study of ciliogenesis in developing epidermis and trachea in the embryo of *Xenopus laevis*. *Am. J. Anat.* 122:19–55.

Sung, C.H., C. Makino, D. Baylor, and J. Nathans. 1994. A rhodopsin gene mutation responsible for autosomal dominant retinitis pigmentosa results in a protein that is defective in localization to the photoreceptor outer segment. *J. Neurosci.* 14:5818–5833.

Tai, A.W., J.Z. Chuang, C. Bode, U. Wolfrum, and C.H. Sung. 1999. Rhodopsin's carboxy-terminal cytoplasmic tail acts as a membrane receptor for cytoplasmic dynein by binding to the dynein light chain Tctex-1. *Cell.* 97:877–887.

Tam, B.M., O.L. Moritz, L.B. Hurd, and D.S. Papermaster. 2000. Identification of an outer segment targeting signal in the COOH terminus of rhodopsin using transgenic *Xenopus laevis*. *J. Cell Biol.* 151:1369–1380.

Tam, B.M., O.L. Moritz, and D.S. Papermaster. 2004. The C terminus of peripherin/rds participates in rod outer segment targeting and alignment of disk incisures. *Mol. Biol. Cell.* 15:2027–2037.

Tam, B.M., G. Xie, D.D. Oprian, and O.L. Moritz. 2006. Mislocalized rhodopsin does not require activation to cause retinal degeneration and neurite outgrowth in *Xenopus laevis*. *J. Neurosci.* 26:203–209.

van Meer, G., D.R. Voelker, and G.W. Feigenson. 2008. Membrane lipids: where they are and how they behave. *Nat. Rev. Mol. Cell Biol.* 9:112–124.

Whitaker, S.L., and B.E. Knox. 2004. Conserved transcriptional activators of the *Xenopus* rhodopsin gene. *J. Biol. Chem.* 279:49010–49018.

Williams, D.S. 2004. Photoreceptor cell biology and inherited retinal degenerations. *In* Recent Advances in Human Biology, vol. 10. C.E. Oxnard, editor. World Scientific Publishing Co. Pte. Ltd., River Edge, NJ. 1–5, 29–107.

Zhang, H., S. Li, T. Doan, F. Rieke, P.B. Detwiler, J.M. Frederick, and W. Baehr. 2007. Deletion of PrBP/delta impedes transport of GRK1 and PDE6 catalytic subunits to photoreceptor outer segments. *Proc. Natl. Acad. Sci. USA.* 104:8857–8862.

Table S1. **Detailed description of R9AP–syntaxin 3 chimeric molecules**

Construct	Cartoon	Residues from R9AP	Residues from Stx3	Figure
Myc-R9AP		1–251	—	Fig. 6 A
Myc-Stx 3		—	1–286	Fig. 6 B
Myc-R9AP/Stx $3_{(TM)}$		1–226	257–286	Fig. 6 C
Myc-Stx 3/R9AP$_{(SH)}$		129–218	1–161 and 259–286	Fig. 6 D
Myc-Stx 3/R9AP$_{(TM)}$		265–285	1–264	Fig. 6 E
Myc-R9AP/Stx $3_{(SH)}$		1–127 and 231–251	162–263	Fig. 6 F

Table S2. **Predicted length of transmembrane domains used in this study**

Construct Name	Sequence	Domain length	Figure
GFP-R9AP TM	GFP_DGQ**LIVSLLLCGTALVAITL**YSIL	17	Figs. 3 D and 9 A
GFP-R9AP TM shorter (−2)	GFP_DGQ**LIVLLCGTALVAITL**YSIL	15	Fig. 9 B
GFP-R9AP TM shortest (−4)	GFP_DGQ**LIVLLCGTALAIL**YSIL	13	Fig. 9 C
GFP-mGluR1 tmd 1	GFP_**IIAIAFSCLGILVTLFVTLIFVLY**RDTPVV	24	Fig. 7
GFP-Cyt b5 TM	GFP_SWWTNW**VIPAISALAVALMY**RLYMAED	14	Fig. 8 A
GFP-Cyt b5 TM longer (+4)	GFP_SWWTNW**VIPAILSLVALLAVALMY**RLYMAED	18	Fig. 8 B
GFP-BclXL TM	GFP_RKGQERFNRWFL**TGMTVAGVVLLGS**LFSRK	13	Fig. 8 C
GFP-BclXL TM K233S	GFP_RKGQERFNRWFL**TGMTVAGVVLLGS**LFSR<u>S</u>	13	Fig. 8 D
GFP-BclXL TM K233S, longer (+4)	GFP_RKGQERFNRWF**LTGMTVALLLLGVVLLGSL**FSR<u>S</u>	19	Fig. 8 E
GFP-Stx 3 TM	GFP_DARRKK**IMILICCVILAIVIASTI**GGIFA	18	Figs. 4 D and 10

The residues shown in bold are predicted to form each respective transmembrane domain as calculated using the DAS server (Cserzo, M., E. Wallin, I. Simon, G. von Heijne, and A. Elofsson. 1997. *Protein Eng.* 10:673–676). The position of the K233S point mutation in BclXL is underlined.